Molecular Crystals and Liquid Crystals

Publication details, including instructions for authors and subscription information:
http://www.tandfonline.com/loi/gmcl20

Characterization of Tungsten Trioxide Thin Film Deposited by Spin Coating and the Effect on Their Insertion in Liquid Crystal Cells

M. Castriota [a], S. Marino [a], C. Versace [a], G. Strangi [a], N. Scaramuzza [a] & E. Cazzanelli [a]

[a] LICRYL - INFM (Liquid Crystal Regional Center) c/o Department of Physics, University of Calabria, Rende (CS), Italy

Version of record first published: 31 Aug 2006

To cite this article: M. Castriota, S. Marino, C. Versace, G. Strangi, N. Scaramuzza & E. Cazzanelli (2005): Characterization of Tungsten Trioxide Thin Film Deposited by Spin Coating and the Effect on Their Insertion in Liquid Crystal Cells, Molecular Crystals and Liquid Crystals, 429:1, 237-253

To link to this article: http://dx.doi.org/10.1080/15421400590930980

Mol. Cryst. Liq. Cryst., Vol. 429, pp. 237–253, 2005

ISSN: 1542-1406 print/1563-5287 online
DOI: 10.1080/15421400590930980

Taylor & Francis
Taylor & Francis Group

Characterization of Tungsten Trioxide Thin Film Deposited by Spin Coating and the Effect on Their Insertion in Liquid Crystal Cells

M. Castriota
S. Marino
C. Versace
G. Strangi
N. Scaramuzza
E. Cazzanelli
LICRYL - INFM (Liquid Crystal Regional Center) c/o Department of Physics, University of Calabria, Rende (CS), Italy

The asymmetric insertion of oxide layers having mixed conduction properties (ionic and electronic) in liquid crystal cells induce various kinds of electro-optical response of the liquid crystals, and this behaviour has been related to the structural differences of the inserted films. In this work, is reported a structural study of such oxide films deposited on indium tin oxide (ITO) covered glasses. To have further confirmations of the model and a better understanding of the basic mechanism underlying the rectification effect and the connections with the structural and electrical properties of the films, WO_3 layers have been studied before and after thermal. Moreover the gelification via spin-coating, has been implemented and the optimization test of various relevant parameters have been performed. The chemical, structural and optical evolution has been extensively investigated as a function of the thermal annealing treatment, by performing vibrational spectroscopy analysis (micro-Raman and IR) impedance spectroscopy characterization and spectroscopic ellipsometry, before testing the films into the NLC cells.

Keywords: electro-optical response; nematic liquid crystals; spectroscopic ellipsometry; tungsten trioxide; vibrational spectroscopy

The authors are indebted to Tiziana Barone and Giuseppe De Santo for their technical assistance to the vibrational spectroscopy measurements. The present investigations have been done in the framework of the Italian MIUR research project "Piani di Potenziamento della Rete Scientifica e Tecnologica" Cluster No. 26-P4.

Address correspondence to M. Castriota, E-mail: castriota@fis.unical.it

1. INTRODUCTION

Few years ago a new method has been developed to achieve the polarity-sensitive electro-optical response in nematic [1,2] and ferroelectric [3] liquid crystal cells, based on the insertion of a mixed conduction (ionic and electronic) film as electrode. The transparent materials matching such requirements are, in principle, the same widely studied in the last years for the electrochromic applications. In fact the first material inserted in nematic liquid crystal (NLC) cells was the tungsten trioxide (WO_3) [1,2], the most used active electrochromic oxide. A quantitative model has been developed [4] to explain the interaction between the WO_3 oxide film and the liquid crystal by the formation of charged layers at the interface, giving rise to a reverse internal electric field, which counteracts the reorientation of NLC molecules (Freedericksz transition). In this case the effect can be ascribed to mobile protons always present in these films [5], but for other oxide films, for instance mixed titania-vanadia films grown by sol-gel route, a more complex behaviour has been observed, i.e., the rectification effect changes its sign after different annealing treatments on the films and seems also to depend on the chemical details of the sol-gel process [6–8].

To have further confirmations of the model and a better understanding of the basic mechanism underlying the rectification effect and the connections with the structural and electrical properties of the films, WO_3 layers have been studied before and after thermal. Moreover the gelification via spin-coating has been implemented and the optimization tests of various relevant parameters have been performed. The chemical, structural and optical evolution has been extensively investigated as a function of the spinning rate and of the thermal annealing treatment, by performing vibrational spectroscopy analysis (micro-Raman and IR) and spectroscopic ellipsometry, before testing the films into the NLC cells.

2. EXPERIMENTAL

2.1. Film Synthesis

The ITO-coated glasses used as substrates were ultrasonically cleaned in acetone, then in bidistilled water and finally in isopropanol and then drying with warm air [9].

Tungsten trioxide sol-gel route is reported in Ref. [10–11]. Briefly, $WOCl_4$ was dissolved in dry isopropanol in Glove Box; with concentration of water and oxygen less than 0.1 ppm and after stirring for one night the solution was used for coating [12].

Different spinning rate, between 600 and 7800 rpm have been tested for coating and here is reported the analysis done on the films obtained at 1200 rpm.

2.2. Raman Spectroscopy

A Raman microprobe Jobin-Yvon Labram was used equipped with a CCD detector and a He-Ne laser (632.8 nm emission). In all the experiments the power of the laser out of the objective (a 100x Mplan Olympus with Numerical Aperture of 0.90) was about 5 mW, and the focused laser spot had about 2–3 μm of apparent diameter. By assuming such values of spot diameter and laser power, we have for the unfiltered laser beam an irradiance of the order of 50–100 kW/cm^2 on the spot. To avoid unwanted laser-induced crystallizations, proper neutral filter were often used, having Optical Density 3, 2, 1, 0.6 and 0.3, corresponding to transmitted laser power fractions of 1/1000, 1/100, 1/10, 1/4 and 1/2, respectively.

2.3. Impedance Measurements Equipment

The bulk electrical conductivity of these oxides is usually quite low and they act as insulators. In general the electric properties of thin films can strongly depend on several factors: the thickness of the film, the initial structure and the eventual structural changes due to thermal treatments. The electric properties of the films have been investigated by using an impedance analyzer (Eg&G 273 A). The distance between the sample connectors pointed on the film was $\sim$5 mm. One connector acts as working electrode, while the counter electrode has been short circuited with the reference one. To avoid short circuit through the ITO layer, tin platelets have been used as contacts on the film surface. In this paper will be shown the trend of the impedance versus frequency because we are mainly interested to the change of the frequency response (shift of cut-off frequency).

2.4. Application of the Films to Liquid Crystal Cells

ITO-coated glasses were used in NLC cells as counter electrode with respect to the electrode spin-coated with the WO_3 gel, playing the role of working electrode. After a careful cleaning in chromic mixtures and repeated cleansing with acetone, they were covered with polyimmide and underwent a rubbing process, to insure a better planar alignment of the NLC molecules.

For the working electrodes, on the contrary, no surface treatment has been performed because the rectification effect is supposed to be related to the ionic charge distribution and motion at the oxide-liquid crystals interface. Thus, the insertion of an alignment layer could strongly modify the wanted phenomena. Moreover, the tungsten trioxide layer induced a homogeneously planar alignment of the liquid crystal molecules in all the prepared cells. The two plates were closed in the standard sandwich configuration by using metallic clamps. The thickness of the cells was ensured by stripes of Mylar (8 μm), and the final value was deduced by analyzing the interference patterns in the transmittance spectrum of the empty cell, measured by a spectrophotometer.

The introduction of the liquid crystal in the space enclosed between the asymmetric glass plates was made very slowly to prevent any orientational alignment induced by the flow. The cell was filled with a NLC called *BL001* by Merck (former E7).

2.5. Electrooptic Response of the NLC Cells: Experimental Set-up

Observations of the electro-optical response of the cells, between crossed polarizers, were made by a polarizing microscope Axioskop Pol (Zeiss). The starting orientation of the NLC cell is set to have a maximum of the transmitted light, when placed on the stage of the microscope between crossed polarizers. Videomicroscopy was performed by a 3CCD color camera TCM 112 (GDS Elettronica) connected to a PC equipped to visualize and to capture the images of the samples. The investigation of the transmitted light intensities was carried out by a large area silicon photodiode (Hamamatsu) mounted on the polarizing microscope. The electrical signal proportional to the light intensity was collected by a digital oscilloscope (Tektronics, Mod. TDS 784). We have used both monochromatic light (He-Ne laser, 632) and "white" light (the bulb of the microscope).

Although, the best fringes can be seen with monochromatic light, all the records discussed in this paper have been obtained using white light.

2.6. Ellipsometry Set-up

Spectra of the ellipsometric angles Ψ and Δ were acquired by a J.A Woollam M2000 F rotating compensator ellipsometer (RCE) in the [0.3 μm–1 μm] wavelength range.

A standard experimental set-up for a RCE is reported in (Fig. 1).

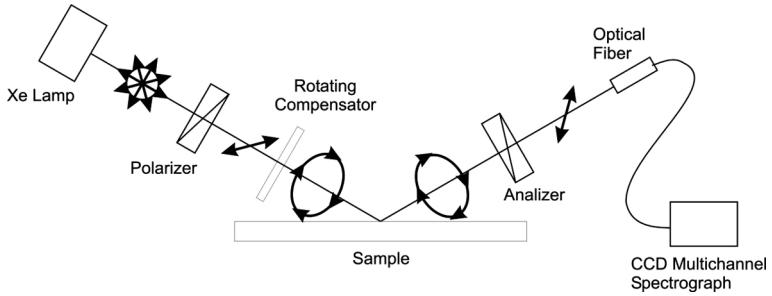

FIGURE 1 Standard experimental set-up for a rotating compensator ellipsometer (RCE).

The state of polarization of the incident white light beam is modulated by the rotating compensator (a $\lambda/4$ waveplate) over the all measurement wavelength range, the interaction with the sample can cause a change in the polarization state of the reflected light beam, which is converted in an intensity modulation projecting the polarization components along the fast axis of the analyzer. The ratio $\rho = \frac{r_p}{r_s} = \tan(\Psi)e^{i\Delta}$ of the Fresnel reflection coefficients r_p and r_s is measured detecting the DC offset at the same time as the 2nd and the 4th harmonics of the Fourier transform of the transmitted light intensity [13].

Ellipsometric spectra (SE) have been modelled by optical model based on the Bruggman effective medium approximation (BEMA) [14], which assumes that for a mixed composition film each component can be represented by its bulk dielectric function. This procedure model the sample by a layer stack, each layer can be completely described by its thickness, complex dielectric function and composition, which are determined by a fitting routine (Levenberg-Marquardt).

3. RESULTS

The thin film of tungsten oxide obtained by spin coating constitute an amorphous layer, containing water molecules coming from the moisture of the air during and after spin-coating deposition. The annealing at 100°C and 300°C induce some water loss, but the structure is basically unchanged while the highest temperature annealing, at 600°C, on the contrary, induces remarkable change in the films structure, revealed even by microscopic observation, as clearly reported in

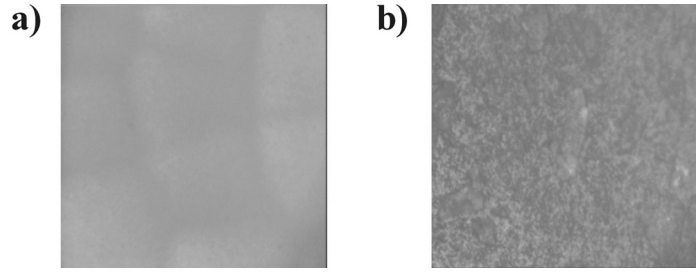

FIGURE 2 Optical image of the Tungsten oxide film a) not annealed b) annealed at 600°C. (See COLOR PLATE XXXI)

(Fig. 2). The grazing angle FT-IR measurements can reveal the existence of the layer in all the conditions, and the spectral changes indicate a significant structural transformation due to 600°C annealing.

Without such treatment, the film is amorphous or nanocrystalline, as indicated by the occurrence of a broad band peaked at 925 cm^{-1}, with a shoulder at about 960 cm^{-1} (see (Fig. 3)). After the 600°C treatment, sharp spectral features typical of ordered crystals are observed.

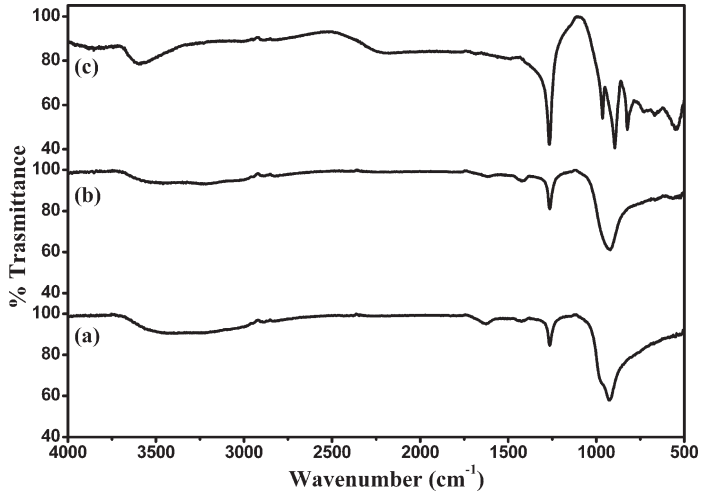

FIGURE 3 Infrared spectra collected on Tungsten Oxide films: (a) annealed at 100°C, (b) annealed at 300°C and (c) annealed at 600°C.

The Raman cross section of such films, "as deposited" or after moderate thermal treatments, must be quite low so that, no appreciable signal can be detected in reasonable times.

On the other hand, for the films annealed at 600°C, the Raman spectra show very sharp peaks at 975, 928, 812 and 312 cm^{-1}, and weaker bands at 302 and 622 cm^{-1}, indicating well crystallized structures (see (Fig. 4)): the resulting ordered phase does not correspond, however, to the standard bulk WO_3. The higher frequency values of the strong Raman peaks suggest, on the contrary, an attribution to vibrations of terminal W-O bonds. The sharpness of the Raman lines together with the visual evidence given in (Fig. 2b) indicates an average

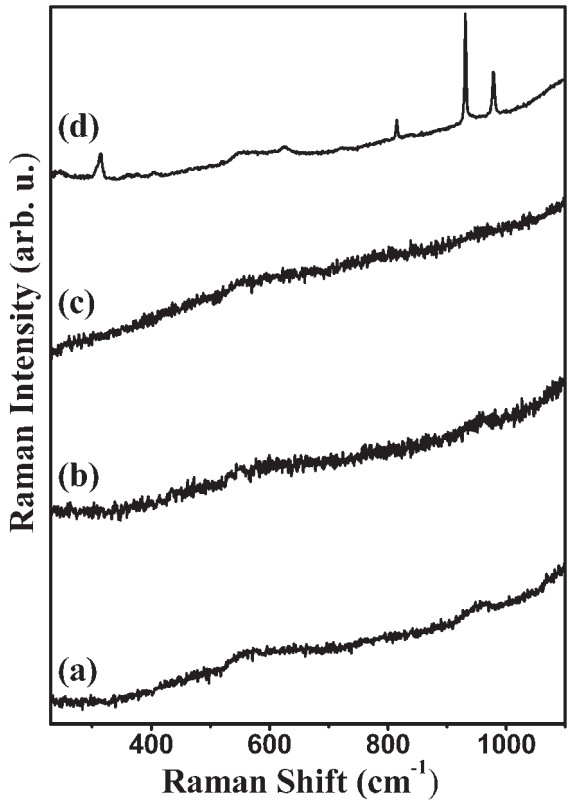

FIGURE 4 Raman spectra collected on Tungsten Oxide samples (a) not annealed, (b) annealed at 100°C, (c) annealed at 300°C and (d) annealed at 600°C.

domain size around one micron. A more detailed discussion of these data will be reported elsewhere; it is worth, within the aims of the present work to remark the occurrence of a crystallization process, also indicated by the IR measurements.

3.1. Electrooptic Response

Asymmetric NLC cell, assembled as described above, have been tested to monitor the evolution of the electrooptic response as a function of the thermal treatment of the inserted tungsten trioxide layer (Fig. 5).

The most interesting fact is the decrease of the rectification effect on the electrooptic response of the cell when the WO_3 film was previously annealed at 300°C, while a full recovery of the effect is observed for film undergoing a higher temperature annealing at 600°C, but the sign of the effect is inverted. The inhibition of the optical switching of NLC layer occurs for the anodic polarization of the WO_3 -coated electrode in the case of "as deposited" or moderately annealed films, confirming the results previously observed [1,2] on similar cells containing WO_3 films deposited by magnetron sputtering; on the contrary, the same inhibition of the switching, associated to the maximum transmittance of light between the crossed polarizers, occurs during the phase of cathodic polarization of the plate electrode annealed at the highest temperature, suggesting the hypothesis of a change of sign of the dominant charge carriers.

As clearly observed in Figure 5, the rectified square wave response is very neat in the two extreme cases (see Figs. 5a and 5c), while it is partial and overlapped to a non-rectified, impulsive response, typical of the usual symmetric cells, for the intermediate annealing case (see Fig. 5b). This behaviour suggests that a decrease of charge carriers number or conductivity occurs in such case for the films, without great associated structural transformation, as suggested by the vibrational spectroscopy data.

3.2. Impedance Spectroscopy

Direct measurements of the thin film impedance give a rough confirmation about the change of conductivity of the films, as a function of the annealing temperature. Even taking into account the difficulty of comparison for absolute conductivity value between different samples, it is clear that an appreciable decrease of electric conductivity occurs for the films undergoing intermediate treatment at 300°C, as

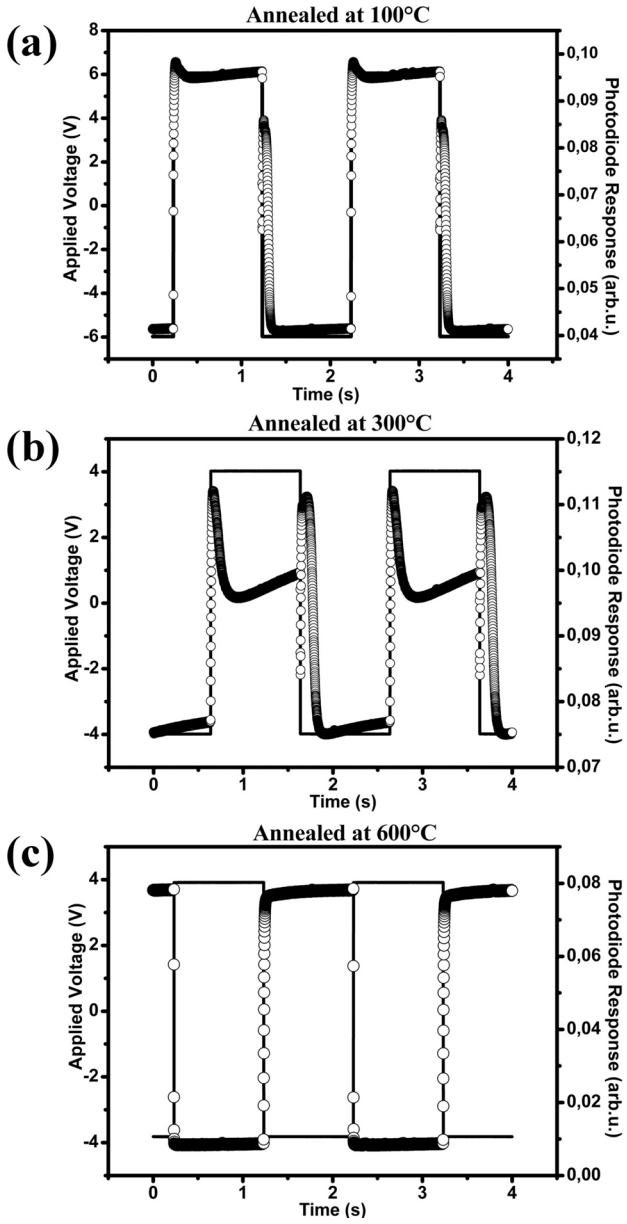

FIGURE 5 Photodiode Response (open circle) of NLC Cells with inserted as electrode WO_3 films, annealed at 100°C (a), at 300°C (b) and at 600°C (c). The solid line is the applied voltage.

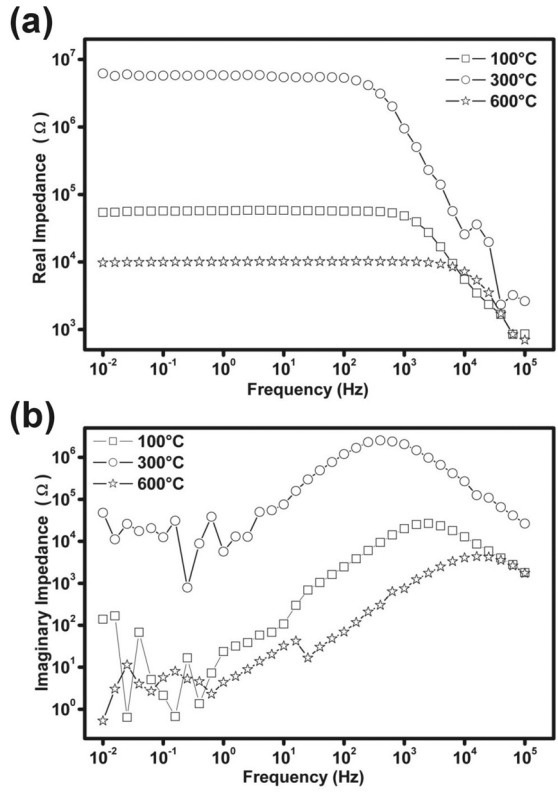

FIGURE 6 Real part (a) and imaginary part (b) of the impedance of the tungsten oxide films annealed at different temperature.

it can be seen from the Bode plot of real part of impedance reported in (Fig. 6) for three typical films. Moreover the maximum of the imaginary part shifts for more than one frequency decade after the 600°C thermal treatment suggesting some changes with regards to the prevalent charge carriers.

3.3. Ellipsometry

The fitting ellipsometric model seems to indicate also the formation of a conducting layer with Drude-like electrons, and this fact is consistent with the observed inversion of the rectification effect in the NLC cell based on these annealed tungsten oxide films.

The spectroscopic ellipsometry reveals also a great transformation after the annealing at 600°C, but the models of layer distributions used to fit the ellipsometric data depict a more complex situation.

To obtain the fitting ellipsometric model of the tungsten oxide films was necessary to have a good model of the ITO-glass substrates. Some value of the refractive index and the extinction coefficient of the float glass have been given by the manufacturer (Balzers S.p.A.) and these values have been used in the modelling procedure. The ITO films were modelled by the superposition of two layers, each of them were described by a combination of two Lorenz oscillators by the relation:

$$\varepsilon(\mathrm{E}) = \varepsilon_\infty + \sum_{\mathrm{k}=1}^{\mathrm{N}} \frac{\mathrm{A_k}}{\mathrm{E_k^2} - \mathrm{E}^2 - \mathrm{i}\Gamma_\mathrm{i}\mathrm{E}}$$

where E is the energy of the incident photons, ε_∞ is the real part of the dielectric function when $\mathrm{E} \to \infty$, $\mathrm{A_k}$ is the strength expressed in

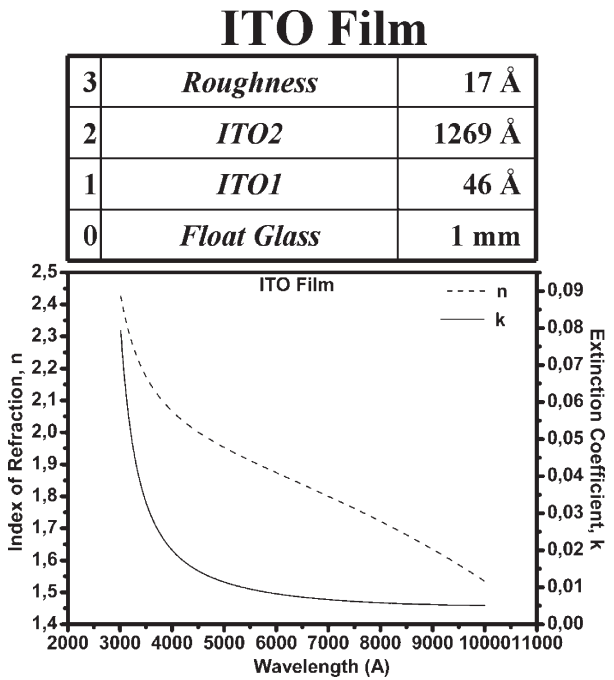

FIGURE 7 Scheme of the model and the optical constants dispersion curves of ITO-glasses substrate.

eV^2, Γ_k is the broadening in eV end E_k is the central energy of the k-th oscillator. In (Fig. 7) are shown the scheme of the model and the optical constants dispersion curves obtained by comparing experimental ellipsometric data with those resulting from the BEMA model simulation by a standard fitting routine.

In this case as well as for all the other samples analysed in this work all the long straightforward intermediate steps of the fitting procedure are omitted for brevity. Also the detailed values of all the fitting parameters (Lorenz oscillator or Cauchy dispersion parameters) for all the resulting layer of any samples are not reported here. However the reader interested to such details can require to the authors more exhaustive information about ellipsometric data elaborations.

The next step was the construction of a tungsten trioxide model. In (Fig. 8) is reported the BEMA model of the not annealed WO_3 coated

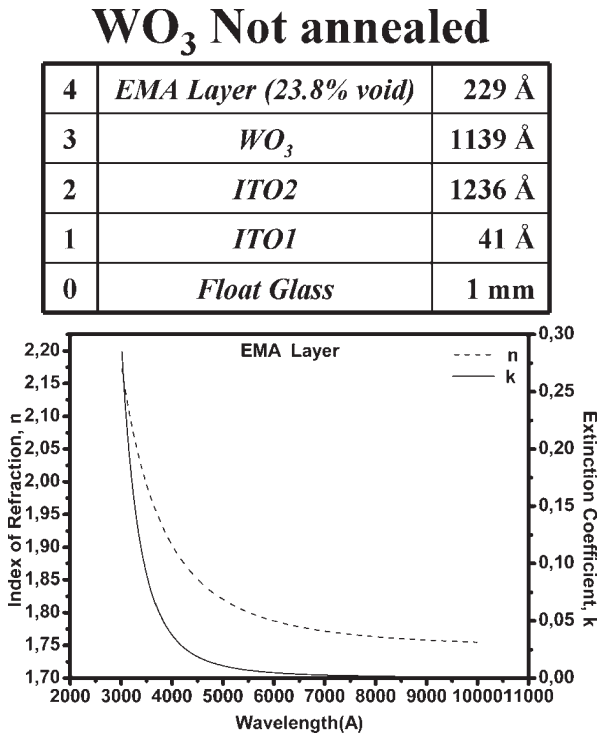

FIGURE 8 Bruggman effective medium approximation (BEMA) model of the not annealed WO_3 coated substrate.

substrates. Film roughness has been modelled by an effective medium approximation (EMA) layer and WO_3 film was parameterized by a Cauchy layer according to:

$$n(\lambda) \cong A + \frac{B}{\lambda^2} + \frac{C}{\lambda^4}$$

The EMA layer mixes the optical constants of the surface Cauchy layer with those of the vacuum, so that this layer can be considered as a suspension of air bubble dispersed in the Cauchy material.

By annealing the film a thinner and denser film configuration is obtained, but the basic character of the films do not change, as confirmed also by the other kind of measurements. In Figures 9–11 are shown the BEMA models of the annealed films along with the optical constant dispersions of the WO_3 annealed films The model not longer holds for films that have been annealed at T = 600°C (Fig. 11), in fact,

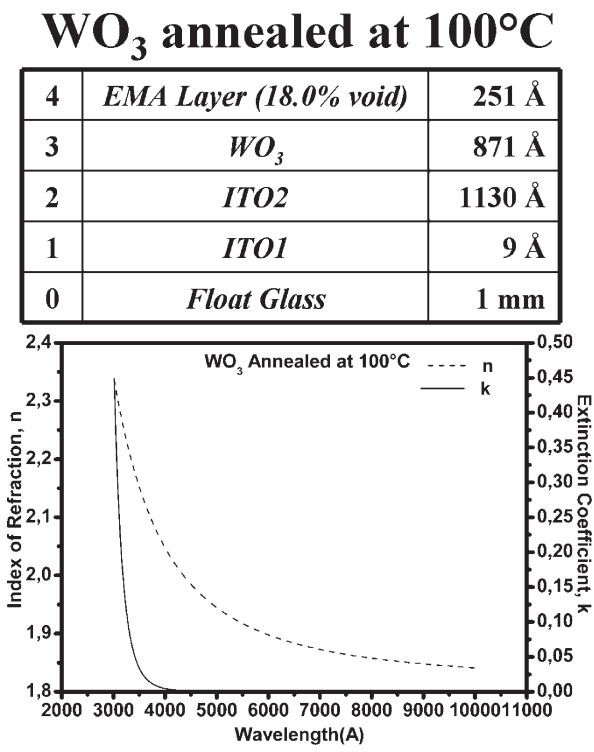

FIGURE 9 Bruggman effective medium approximation (BEMA) models of the annealed at 100°C WO_3 coated substrate.

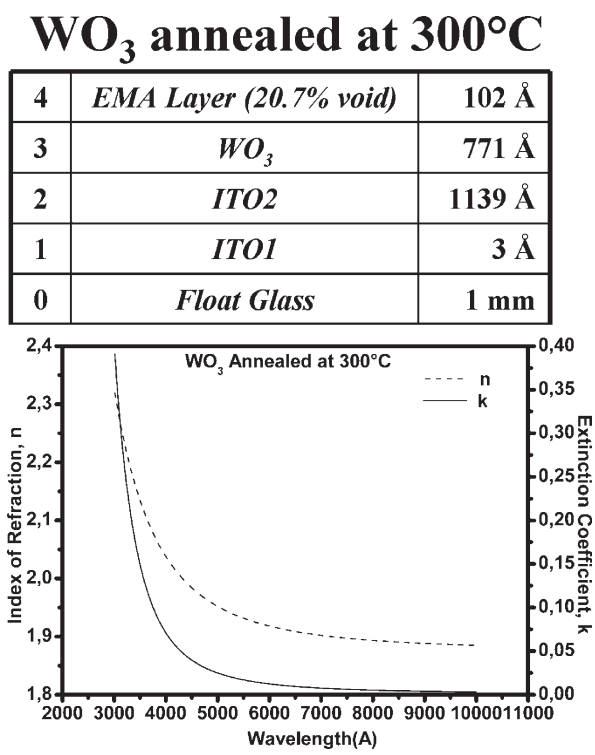

FIGURE 10 Bruggman effective medium approximation (BEMA) models of the annealed at 300°C WO_3 coated substrate.

in this case a new layer must be inserted at the ITO-WO_3 interface, which can be described by a two Lorenz oscillator model, having one of the energies close to zero, so that a Drude –like model can be adopted.

4. CONCLUSIONS

The comparison of the impedance, ellipsometric and vibrational spectroscopic data on the spin-coated films of tungsten oxide and the observed electrooptic behaviour of the NLC cells where such films are inserted, confirm basically the models previously developed to explain the rectification effect of the oxide layers on the liquid crystal switching.

The "as deposited" films of tungsten oxide present a good protonic conduction, so that these positive charge carriers build up an interface double layer during the anodic polarization of the cell, and induces the

WO_3 annealed at 600°C

5	*EMA Layer (29.4% void)*	428 Å
4	*WO_3*	268 Å
3	*Drude layer*	100 Å
2	*ITO2*	1273 Å
1	*ITO1*	1 Å
0	*Float Glass*	1 mm

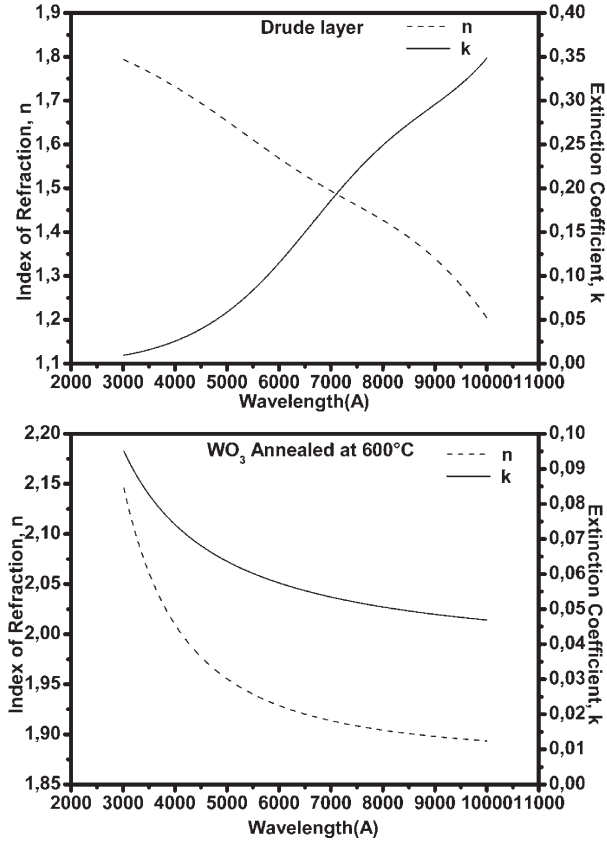

FIGURE 11 Bruggman effective medium approximation (BEMA) models of the annealed at 600°C WO_3 coated substrate.

internal effective field inhibiting the NLC electrooptic switching, while those undergoing moderate thermal treatments present a complex intermediate configuration. In fact the rectification effect decreases, in good agreement with the protonic mobility decrease, after the 300°C annealing. It is well known that at about such temperature the water molecules leave the amorphous structure of the WO_3 films, but the transition to a crystalline compacted phase occurs only for higher temperature treatments [15]; furthermore, the extending crystalline order after dehydration do not improve the protonic conductivity, while enhancing remarkably the electronic conductivity of such film, as demonstrated by coloring experiments after different annealing temperatures [16]. The absence of Raman signal and the results from the ellipsometric model fitting confirm the similarity of the film annealed at 100°C and those annealed at 300°C: no great structural modification takes place for such treatments up to 300°C and the basic structure is still amorphous, with a thickness of about 100 nm.

On the contrary, the 600°C annealing induces the formation of anhydrous ordered phases, as revealed by the IR and Raman spectral changes, and a remarkable increase of the electrical conductivity, as indicated by the impedance measurements. The change of sign of the electrooptic rectification effect seems to suggest a change of sign of the prevalent charge carriers, in agreement with impedance data and previous findings [16]. The fitting ellipsometric model seems also to indicate the formation of a conducting layer with Drude-like electrons, and this fact is consistent with all the other experimental data indicating an increase of electronic conductivity.

Further studies, focused on the influence of the film thickness, as well as of the chemical and thermal history, seem to be necessary to better characterize the structural transformation and the change of the electric proprieties of such material and their consequence on the electrooptic response when inserted into NLC cells.

REFERENCES

[1] Strangi, G., Lucchetta, D. E., Cazzanelli, E., Scaramuzza, N., Versace, C., & Bartolino, R. (1999). *Applied Physics Letters, 74*(4), 534.
[2] Cazzanelli, E., Scaramuzza, N., Strangi, G., Versace, C., Pennisi, A., & Simone, F. (1999). *Electrochimica Acta, 44*(18), 3101.
[3] Strangi, G., Versace, C., Scaramuzza, N., & Bruno, V. (2002). *J. Appl. Phys., 92*(7), 3630.
[4] Alexe-Ionescu, A. L., Th. Ionescu, A., Scaramuzza, N., Strangi, G., Versace, C., Barbero, G., & Bartolino, R. (2001). *Physical Review, E 64*, 011708–1.

[5] Strangi, G., Cazzanelli, E., Scaramuzza, N., Versace, C., & Bartolino, R. (2000). *Phys. Rev, E 62*(2), 2263.
[6] Bruno, V., Cazzanelli, E., Scaramuzza, N., Strangi, G., Ceccato, R., & Carturan, G. (2002). *J. Appl. Phys., 92*(9), 5340.
[7] Cazzanelli, E., Marino, S., Bruno, V., Castriota, M., Scaramuzza, N., Strangi, G., Versace, C., Ceccato, R., & Carturan, G. (2003). *Solid State Ionics, 165*, 201.
[8] Marino, S., Castriota, M., Bruno, V., Cazzanelli, E., Strangi, G., Versace, C., & Scaramuzza, N. *Electro-Optical investigations of nematic liquid crystal cells containing Titania-Vanadia thin films prepared by sol-gel synthesis*, Submitted to *J. Appl. Phys.*
[9] Ozer, N. & Lampert, C. M. (1999). *Thin Solid Films, 349*, 205.
[10] Ozer, N. (1997). *Thin Solid Films, 304*, 310.
[11] Livage, J. & Ganguli, D. (2001). *Solar Energy Materials & Solar Cells, 68*, 365.
[12] Krings L. H. M. & Talen, W. (1998). *Solar Energy Materials & Solar Cells, 54*, 27.
[13] Timson, A. J., Spencer-Smith, R. D., Alexander, A. K., Greef, R., & Frey, J. G. (2003). *Meas. Sci. Technol., 14*, 508.
[14] Aspnes, D. E. (1982). *Thin Solid Films, 89*, 249.
[15] Agrawal, A. & Habibi, H. (1989). *Thin Solid Films, 169*, 257.
[16] Antonaia, A., Polichetti, T., Addonizio, M. L., Aprea, S., Minarini, C., & Rubini, A., (1999). *Thin Solid Films, 354*, 73.